Check for updates

Rapid and sensitive determination of residual prion infectivity from prion-decontaminated surfaces

Sara M. Simmons,[1] Vivianne L. Payne,[2] Jay G. Hrdlicka,[1] Jack Taylor,[3] Peter A. Larsen,[4,5] Tiffany M. Wolf,[5,6] Marc D. Schwabenlander,[4,5] Qi Yuan,[1] Jason C. Bartz[1,5,7]

AUTHOR AFFILIATIONS See affiliation list on p. 17.

ABSTRACT Prion diseases are untreatable fatal transmissible neurodegenerative diseases that affect a wide range of mammals, including humans, and are caused by PrP^{Sc}, the infectious self-templating conformation of the host-encoded protein, PrP^C. Prion diseases can be transmitted via surfaces (e.g., forceps, EEG electrodes) in laboratory and clinical settings. Here, we use a combination of surface swabbing and real-time quaking-induced conversion (RT-QuIC) to test for residual surface-associated prions following prion disinfection. We found that treatment of several prion-contaminated laboratory and clinically relevant surfaces with either water or 70% EtOH resulted in robust detection of surface-associated prions. In contrast, treatment of surfaces with sodium hypochlorite resulted in a failure to detect surface-associated prions. RT-QuIC analysis of prion-contaminated stainless steel wires paralleled the findings of the surface swab studies. Importantly, animal bioassay and RT-QuIC analysis of the same swab extracts are in agreement. We report on conditions that may interfere with the assay that need to be taken into consideration before using this technique. Overall, this method can be used to survey laboratory and clinical surfaces for prion infectivity following prion decontamination protocols.

IMPORTANCE Prion diseases can be accidentally transmitted in clinical and occupational settings. While effective means of prion decontamination exist, methods for determining the effectiveness are only beginning to be described. Here, we analyze surface swab extracts using real-time quaking-induced conversion (RT-QuIC) to test for residual prions following prion disinfection of relevant clinical and laboratory surfaces. We found that this method can rapidly determine the efficacy of surface prion decontamination. Importantly, examination of surface extracts with RT-QuIC and animal bioassay produced similar findings, suggesting that this method can accurately assess the reduction in prion titer. We identified surface contaminants that interfere with the assay, which may be found in clinical and laboratory settings. Overall, this method can enhance clinical and laboratory prion safety measures.

KEYWORDS prion disease, prion decontamination, prion surveillance

P rion diseases are fatal, neurodegenerative disorders that affect several mammalian species. Human prion diseases include Creutzfeldt-Jakob disease (CJD), Gerstmann-Sträussler-Scheinker disease, fatal familial insomnia, and Kuru (1–4). Prion diseases known to afflict other species include chronic wasting disease in cervids, scrapie in sheep and goats, camel prion disease in dromedary camels, and bovine spongiform encephalopathy (BSE) in cattle (5–9). Prion diseases are caused by the misfolding of the normal cellular form of the prion protein (PrP^C) into the infectious and pathogenic form (PrP^{Sc}) (10–15). PrP^{Sc} converts further PrP^C into the pathogenic form eventually leading to neuronal dysfunction and death of the host (16–20). Prion strains are operationally

defined by a heritable phenotype of disease that is encoded by strain-specific conformations of PrP^{Sc} (21–23). Mounting evidence indicates that several other protein misfolding neurodegenerative diseases follow the prion paradigm (24–29). While not contagious in a population, these diseases share similarities in prion formation, spread in the nervous system, and strain-specific phenotypes of the disease (25, 27, 30–37).

Prions are highly resistant to common forms of disinfection. Prions and/or PrP^{Sc} are resistant to inactivation by UV light, ionizing radiation, heat, formaldehyde, hydrogen peroxide, and alcohol (38–48). Similarly, multiple system atrophy α-synuclein and amyloid-β prions are resistant to inactivation by formalin fixation (49–51). Recently, it has been shown that Lewy body α-synuclein prions that cause dementia are resistant to inactivation by autoclaving at 121°C (52). Prions can be chemically inactivated with sodium hydroxide, sodium hypochlorite, acidic sodium dodecyl sulfate, hypochlorous acid, and the phenolic compounds Environ LpH and Wexide-128 (53–59). Importantly, prion strain-specific differences in susceptibility to inactivation by both physical and chemical methods have been observed; therefore, the efficacy of antiprion modalities to new prion diseases or strains must be interpreted with caution (56, 60). Strain-specific incomplete inactivation of prions can result in the emergence of a minor prion strain from a mixture (61).

Prions can be transmitted via iatrogenic infection. Iatrogenic infection can arise from prion-contaminated transplant materials or medical equipment. The first reported case of iatrogenic infection originated from a corneal transplant that was derived from a cadaver unknowingly harboring CJD (62). Additionally, iatrogenic CJD can occur after the transplantation of CJD-contaminated human growth hormone or dura mater (63–73). Iatrogenic Alzheimer's disease in recipients of growth hormone derived from pituitary glands that contain Aβ prions has been observed (36, 74, 75). Cases of iatrogenic CJD transmission have been reported following the use of contaminated neurosurgical tools involved in procedures such as brain biopsies and tumor removals on a patient later diagnosed with CJD (76–80).

Occupational prion transmission has been reported. The first account of an occupational prion transmission occurred in a laboratory worker who was exposed to brain material from humanized transgenic mice infected with sheep-adapted BSE, likely from a puncture wound from forceps (81). A second suspect case of occupational CJD attributed to laboratory transmission was reported in 2021 resulting in a moratorium on prion research in France (82). The reported transmission of non-PrP-based prions from the iatrogenic transmission and laboratory studies, in conjunction with PrP and some non-PrP prions' unusual resistance to inactivation, highlights the potential for prion transmission under occupational and medical settings (83).

Prion decontamination efficacy has been measured through bioassay of treated samples. This can be accomplished by animal bioassay of treated tissue homogenates or prion-coated stainless steel wires (84, 85). While effective, this process is costly and time-consuming (86, 87). The scrapie cell assay (SCA) is as sensitive as animal bioassay, more precise, and can be completed in a fraction of the time (88). The SCA can accurately measure prions on the surface of stainless steel wires to determine the efficacy of prion decontamination methods (89). A weakness of this method is only a limited number of prion strains are compatible with the SCA, and the method is not able to assess for prions on working surfaces in laboratory or clinical settings. Ultra-sensitive prion detection assays, such as real-time quaking-induced conversion (RT-QuIC), have allowed for the amplification and detection of minute amounts of PrP^{Sc} and the prion forms of synuclein, tau and Aβ (90–95). Recent work indicates that PrP, α-synuclein, and tau prions can be detected from media that are applied to a surface (96). Here, we investigate if the combination of RT-QuIC coupled with the newly developed swabbing methodology provides a practical approach to assess surface decontamination efficacy in laboratory and clinical settings (97).

RESULTS

Efficient recovery of prions applied to laboratory surfaces

Each surface type was contaminated with 10-fold serial dilutions of hyper transmissible mink encephalopathy (HY TME)-infected brain homogenate in Dulbecco's phosphate-buffered saline (DPBS) (mother dilutions), and contaminated surfaces were allowed to dry for 24 hours prior to swabbing, extraction, and RT-QuIC analysis (Fig. 1, panel A). Negative control swab extracts failed to yield positive readings, in terms of maxpoint ratio (MPR) above the determined positive threshold of 2. In some instances, however, positive signals were observed in one out of four technical well replicates for one technical negative swab extract replicates. When comparing the SD_{50} (seeding dose that resulted in 50% positivity for tested samples determined by RT-QuIC end-point dilutions, Table 1) of swabbing-recovered HY TME to the original HY TME mother dilutions applied to the surface, there was an approximate loss of 1.1 logs for glass surfaces (Fig. 1, panel
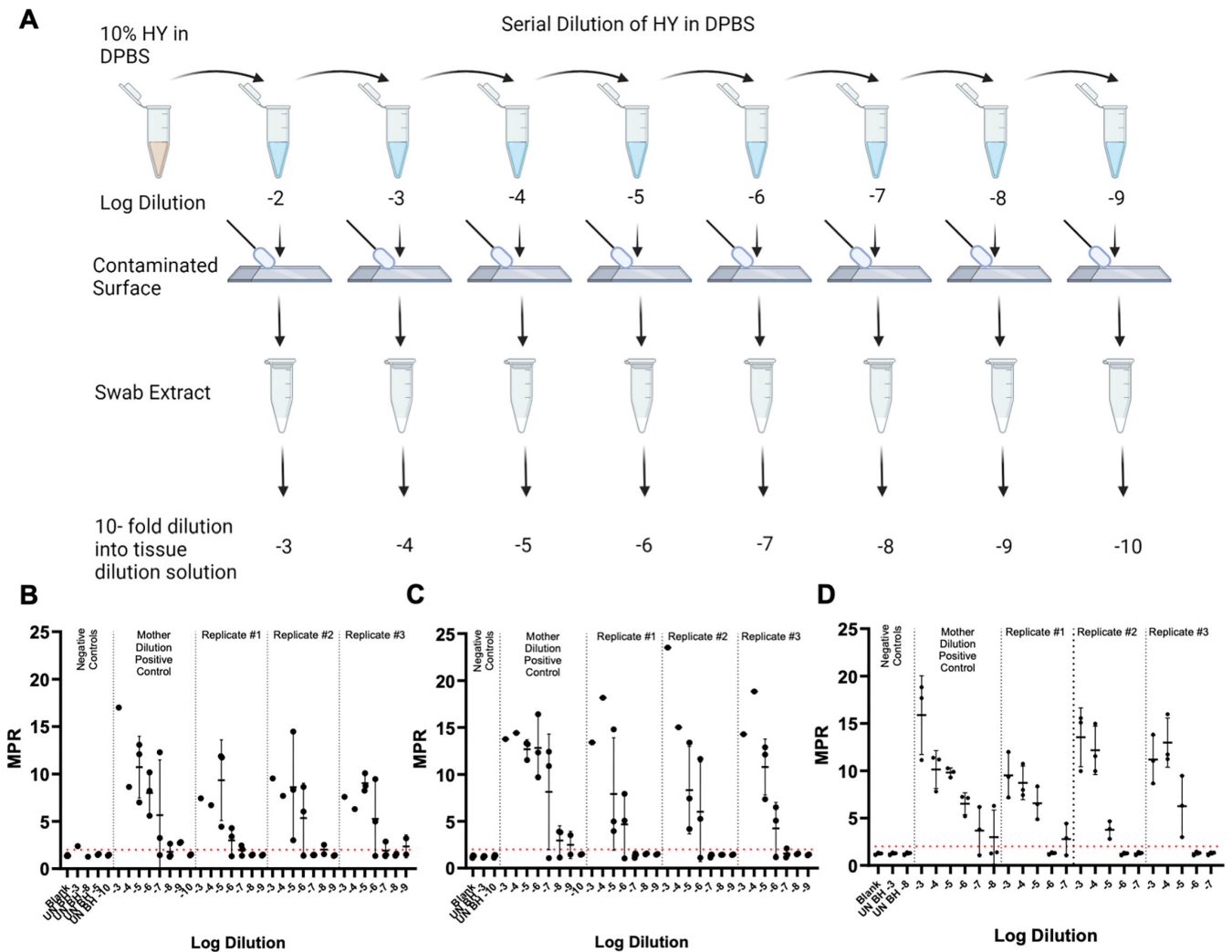

FIG 1 Effective swabbing recovery of prions applied to laboratory surfaces. (A)Vertical dilution method surface contamination and swabbing methodology of contaminated laboratory surfaces. Created with BioRender.com. (B)RT-QuIC detection for glass slide surface-recovered HY prions. (C)RT-QuIC detection for stainless steel surface-recovered HY prions. (D)RT-QuIC detection for laboratory benchtop surface-recovered HY prions. Negative plate controls include blank (tissue dilution solution) and uninfected brain homogenate. A positive fluorescence threshold (illustrated by the red line) was determined to be at 2. The maxpoint ratio reported is the ratio of the maximum fluorescence to the initial fluorescence reading obtained by the plate reader. Each point represents the average MPR from one biological replicate (mean ± standard deviation).

TABLE 1 Comparison of log SD_{50}/g of brain homogenate, determined by RT-QuIC end-point dilutions, of prion-contaminated surface swabbing recovered HY

Surface	Biological replicate	Mother dilution	Technical replicate #1	Technical replicate #2	Technical replicate #3	Technical replicate[a]
Glass slide	#1	10.53	8.93	9.03	9.20	9.05 ± 0.11
	#2	9.33	8.78	9.17	8.92	8.96 ± 0.16
	#3	9.70	8.17	8.03	8.45	8.22 ± 0.17
Stainless steel	#1	10.53	9.03	9.20	9.03	9.09 ± 0.08
	#2	10.53	8.70	9.20	8.70	8.87 ± 0.24
	#3	9.20	7.37	7.70	7.37	7.48 ± 0.16
Benchtop	#1	10.20	8.33	7.37	8.20	7.97 ± 0.43
	#2	9.20	7.70	7.70	7.37	7.59 ± 0.16
	#3	9.44	7.70	6.33	8.03	7.35 ± 0.74

[a]Average ± SD.

B), 1.6 logs for stainless steel surfaces (Fig. 1, panel C), and 2 logs for benchtop surfaces (Fig. 1, panel D), respectively.

Residual bleach does not interfere with RT-QuIC detection of surface-recovered HY TME

The potential inhibitory role of bleach residue that may be introduced to the RT-QuIC reaction from treated surfaces was investigated. Glass slide surfaces were contaminated with 10^{-2} HY TME-infected brain and were allowed to dry for 24 hours prior to bleach treatment, swabbing, extraction, and RT-QuIC analysis (Fig. 2, panel A). To quantify any potential inhibition imparted by bleach residue, the bleach control swab extracts were run in comparison to a representative swab extract that had not undergone treatment. The SD_{50} was determined and used to assess any loss of detection. Negative plate controls failed to yield MPR above the determined positive threshold of 2. (Fig. 2, panel B). The swabbing of residual bleach, followed by swabbing of an additional surface contaminated with 10^{-2} HY TME-infected brain homogenate in DPBS yielded SD_{50} results, determined by RT-QuIC end-point dilutions, that were within 0.2 log when compared to 10^{-2} HY brain homogenate (BH) swab extract samples alone (Table 2). The results of this experiment illustrate that residual bleach, which may be present on a treated surface following thorough rinsing with water, does not inhibit the RT-QuIC reaction. Overall, the reduction of RT-QuIC seeding activity with bleach treatment is a result of decontamination.

Bleach is an effective disinfectant for HY-contaminated laboratory surfaces, while 70% EtOH and H_2O are ineffective disinfectants

The efficacy of multiple disinfectants in decontaminating prion-contaminated surfaces was investigated. These disinfectants included undiluted bleach and 70% EtOH. Water was used as a negative disinfection control. Each surface type was contaminated with 10^{-2} HY TME-infected brain homogenate, and surfaces were allowed to dry for 24 hours prior to disinfection, swabbing, extraction, and RT-QuIC analysis (Fig. 3, panel A). Each disinfectant was applied to the prion-contaminated area for a treatment duration of 10 minutes. Swab extracts were then evaluated with RT-QuIC, and each plate compared an untreated positive surface control extract to surfaces treated with H_2O, 70% EtOH, and undiluted bleach. Negative swab controls failed to yield fluorescence signals above the positive fluorescence threshold determined to be at 2 (Fig. 3, panel B). In rare instances, 1/4 technical replicate wells for negative control swab extracts showed low seeding capabilities. The treatment of glass slides, stainless steel surfaces, and benchtops with undiluted bleach led to a complete loss of fluorescence signals above the positive fluorescence threshold of 2 (Fig. 3, panel C). Treatment of glass slide surfaces with both 70% EtOH and H_2O led to an approximate one log reduction in the SD_{50} when compared

A

1. Surface contaminated with HY in DPBS

2. Surface treated with bleach and rinsed with H_2O.

3. Residual bleach swabbed

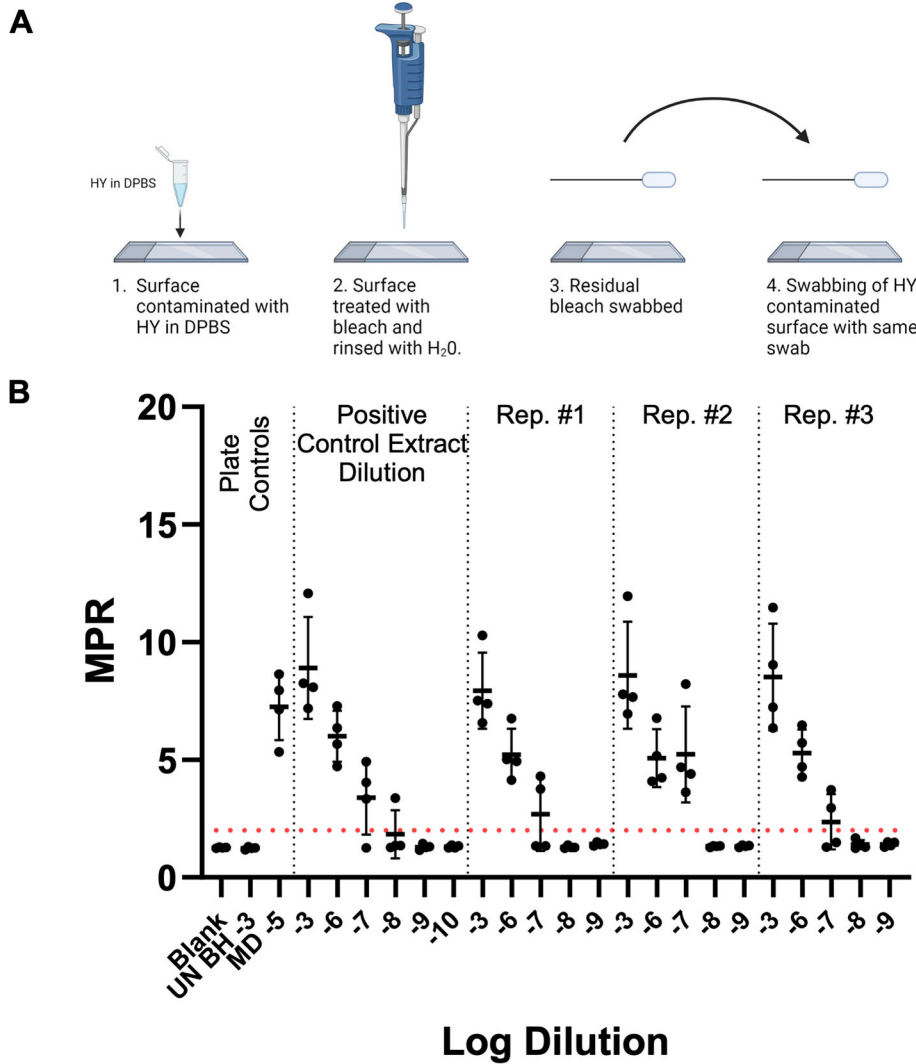4. Swabbing of HY contaminated surface with same swab

B

FIG 2 Residual bleach does not interfere with RT-QuIC detection of surface-recovered prions. (A)Residual bleach swabbing methodology (Created with BioRender.com.). (B)RT-QuIC detection of swab extracts from prion-contaminated surfaces exposed to residual bleach residue. Plate controls included negative plate controls: blank (tissue dilution solution) and uninfected hamster brain homogenate of 10^{-3} and the positive plate control mother dilution 10^{-5}. A positive fluorescence threshold (illustrated by the red line) was determined to be at 2. The maxpoint ratio reported is the ratio of the maximum fluorescence to the initial fluorescence reading obtained by the plate reader (mean ± standard deviation). Each experiment was performed at least three times, with similar results obtained from each experiment.

to the swab extracts of untreated, prion-contaminated glass slide surfaces (Table 2). Treatment of stainless steel surfaces with H_2O did not lead to a statistically significant (0 > 0.05) reduction in SD_{50} when compared to the untreated surface. In addition, there was an approximate 0.5 log reduction in SD_{50} for the 70% EtOH-treated stainless steel surfaces, but this difference was not statistically significant ($P > 0.05$). Seventy percent EtOH and H_2O treatment of benchtop surfaces led to statistically significant ($P < 0.05$) reduction in SD_{50} at approximately 0.7 and 1.3 logs, respectively. Overall, bleach is an effective disinfectant for prion-contaminated surfaces, while H_2O and 70% EtOH are ineffective.

TABLE 2 RT-QuIC detection (log SD$_{50}$/g of brain homogenate as determined by end-point dilutions) of HY recovered from relevant surfaces treated with various disinfectants

Surface	Biological replicate	Technical replicate	Treatment				
			None	H$_2$O	70% EtOH	Bleach	Bleach control
Glass slide	1	a	10.20	10.20	9.20	MPR< 2	10.70
		b	10.47	9.37	9.37	MPR< 2	10.70
		c	11.20	10.20	9.70	MPR< 2	10.20
	2	a	10.93	9.20	9.53	MPR< 2	9.70
		b	10.37	9.37	9.20	MPR< 2	10.20
		c	10.53	8.20	10.03	MPR< 2	9.70
	3	a	9.20	8.33	8.20	MPR< 2	9.47
		b	9.70	8.93	9.33	MPR< 2	9.53
		c	9.20	8.20	9.20	MPR< 2	10.20
	Avg± SD		10.20 ± 0.66	9.11 ± 0.73	9.31 ± 0.47	MPR< 2	10.04 ± 0.44[a]
Stainless steel	1	a	10.53	10.32	9.47	MPR< 2	N/A[b]
		b	10.37	9.70	10.20	MPR< 2	N/A
		c	9.93	9.70	9.37	MPR< 2	N/A
	2	a	9.20	9.30	9.03	MPR< 2	N/A
		b	9.20	8.93	8.70	MPR< 2	N/A
		c	9.37	10.20	9.03	MPR< 2	N/A
	3	a	9.03	10.02	8.20	MPR< 2	N/A
		b	10.03	9.20	9.37	MPR< 2	N/A
		c	8.93	9.20	8.70	MPR< 2	N/A
	Avg± SD		9.62 ± 0.57	9.62 ± 0.46	9.12 ± 0.54	MPR< 2	N/A
Benchtop	1	a	10.93	9.20	10.03	MPR< 2	N/A
		b	10.37	8.70	10.03	MPR< 2	N/A
		c	10.93	9.70	10.20	MPR< 2	N/A
	2	a	10.37	10.03	10.37	MPR< 2	N/A
		b	11.37	9.93	10.20	MPR< 2	N/A
		c	10.70	10.03	10.20	MPR< 2	N/A
	3	a	10.37	8.37	9.37	MPR< 2	N/A
		b	10.37	8.93	10.03	MPR< 2	N/A
		c	10.93	10.03	9.93	MPR< 2	N/A
	Avg± SD		10.70 ± 0.34	9.44 ± 0.61	10.04 ± 0.27	MPR< 2	N/A

[a]Average ± SD.
[b]Not Applicable.

Direct surface measurement of prion seeding activity on stainless steel wire mimics the results of surface-recovered prion seeding activity

Mock-treated, plus HY TME-contaminated stainless steel wires were subjected to treatment with either H$_2$O, 70% EtOH, or undiluted bleach and were subsequently assayed with RT-QuIC in order to test residual infectivity that may remain on the surface itself following treatment (Fig. 4, panel A). Two- to three-millimeter stainless steel wires were incubated with either UN HA BH 10^{-3} or HY 10^{-3} BH for 1 hour followed by thorough rinsing. Both sets of wires were then subjected to treatment with various disinfectants for 10 minutes prior to rinsing and were then added directly to the 96-well plate for assay with RT-QuIC. The treatment of HY-contaminated stainless steel wires with undiluted bleach led to a complete loss of fluorescence signals above the positive fluorescence threshold of 2 (Fig. 4, panel B). In addition, 70% EtOH and H$_2$O were ineffective disinfectants for HY-contaminated stainless steel wires. In addition, negative control wires that underwent the same treatments failed to yield fluorescence signals above the positive fluorescence threshold of 2. All treated HY TME treatment data points are an average of 16 replicate wires, except one biological replicate of 70% EtOH-treated wires, which contained 15 replicate wires, and 1 biological replicate of H$_2$O-treated wires, which contained 14 replicate wires.
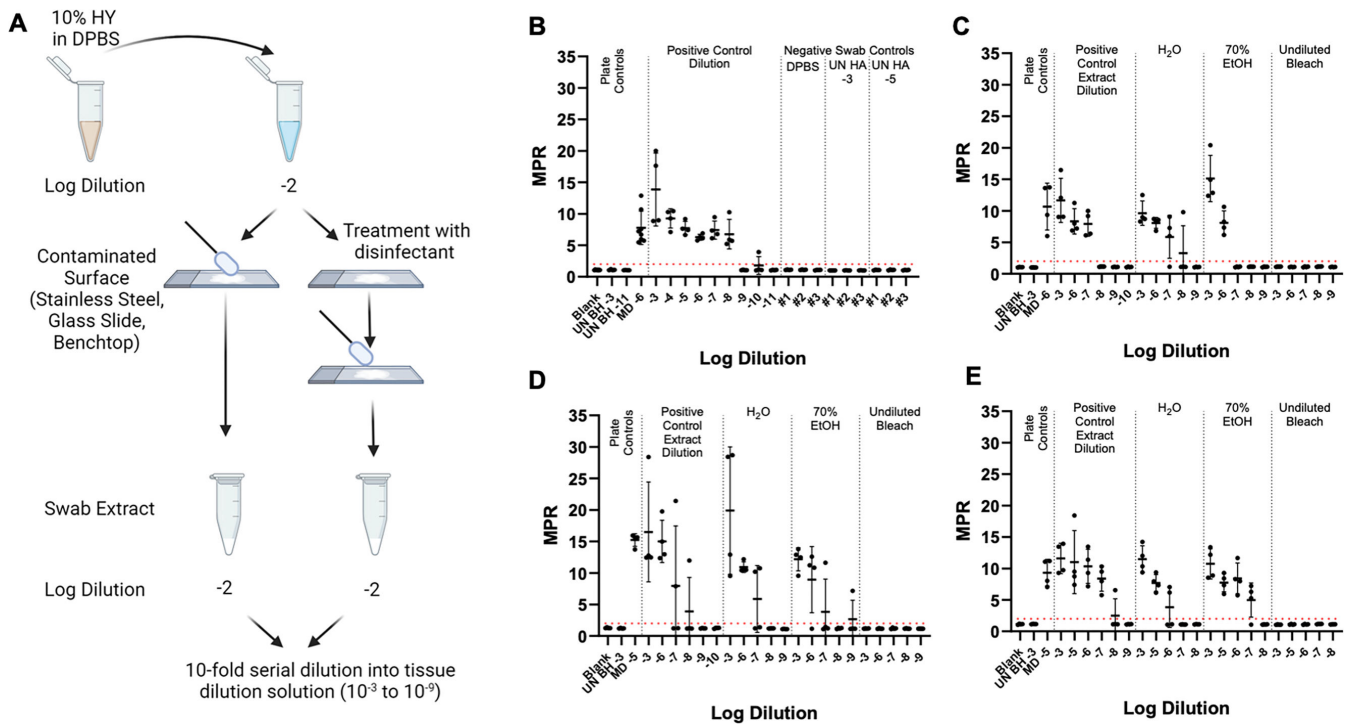
FIG 3 Bleach is an effective disinfectant for HY-contaminated laboratory surfaces, while 70% EtOH and H_2O are ineffective disinfectants. (A)Horizontal dilution method surface contamination and swabbing methodology of contaminated and treated laboratory surfaces (created with BioRender.com). (B)RT-QuIC detection for glass slide surface recovered negative controls included UN HA BH 10^{-3}, UN HA BH 10^{-5}, and DPBS. (C)RT-QuIC detection for swab extracts from HY-contaminated glass slide surfaces treated with H_2O, 70% ethanol, or undiluted bleach for 10 minutes. (D)RT-QuIC detection for swab extracts from HY-contaminated stainless steel surfaces treated with H_2O, 70% ethanol, or undiluted bleach for 10 minutes. (E)RT-QuIC detection for swab extracts from HY-contaminated benchtop surfaces treated with H_2O, 70% ethanol, or undiluted bleach for 10 minutes. Negative plate controls include blank (tissue dilution solution) and uninfected brain homogenate of 10^{-3}. A positive plate control consisted of 10^{-5} or 10^{-6} dilution prepared from the mother dilution applied to surfaces. A positive fluorescence threshold (illustrated by the red line) was determined to be at 2. The maxpoint ratio reported is the ratio of the maximum fluorescence to the initial fluorescence reading obtained by the plate reader (mean ± standard deviation). Each experiment was performed at least three times, with similar results obtained from each experiment.

Examination of swab extracts by RT-QuIC and animal bioassay for prions

Mock-contaminated glass and HY TME-contaminated glass treated with either H_2O, 70% EtOH, or bleach were swabbed, and the swab extract was split into two equal aliquots (Fig. 5, panel A). The first aliquot was analyzed using RT-QuIC for the presence of seeding activity. In the negative control glass surfaces treated with either DPBS, 10^{-3}, or 10^{-5} dilution of uninfected (UN) brain homogenate did not result in detectable RT-QuIC seeding activity (Fig. 5, panel B). Swab extracts from glass surfaces contaminated with HY TME that were treated with either H_2O or 70% EtOH yielded an SD_{50} within approximately 1 log when compared to swab extracts that did not undergo treatment (P = 0.09172). Bleach treatment of contaminated glass surfaces resulted in a complete loss of fluorescence above the defined threshold. The second aliquot was intracerebrally (i.c.) inoculated into hamsters to examine for prion infectivity. As a positive control, hamsters were i.c. inoculated with a 10^{-4} dilution of HY TME-infected brain homogenate resulting in all (n = 5) of the animals developing clinical signs of hyperexcitability and ataxia at 76 ± 3 days post-infection (dpi) (Fig. 5, panel D). As a negative control, swab extract from an uncontaminated glass surface resulted in none (n = 5) of the animals developing clinical signs of prion infection at 300 dpi when the experiment was terminated (Fig. 5, panel D). Swab extracts from HY TME-contaminated surfaces treated with either water or 70% EtOH resulted in all (n = 5) of the animals developing clinical signs of prion disease at 91 ± 7 and 95 ± 4 dpi, respectively. Swab extract from HY TME-contaminated
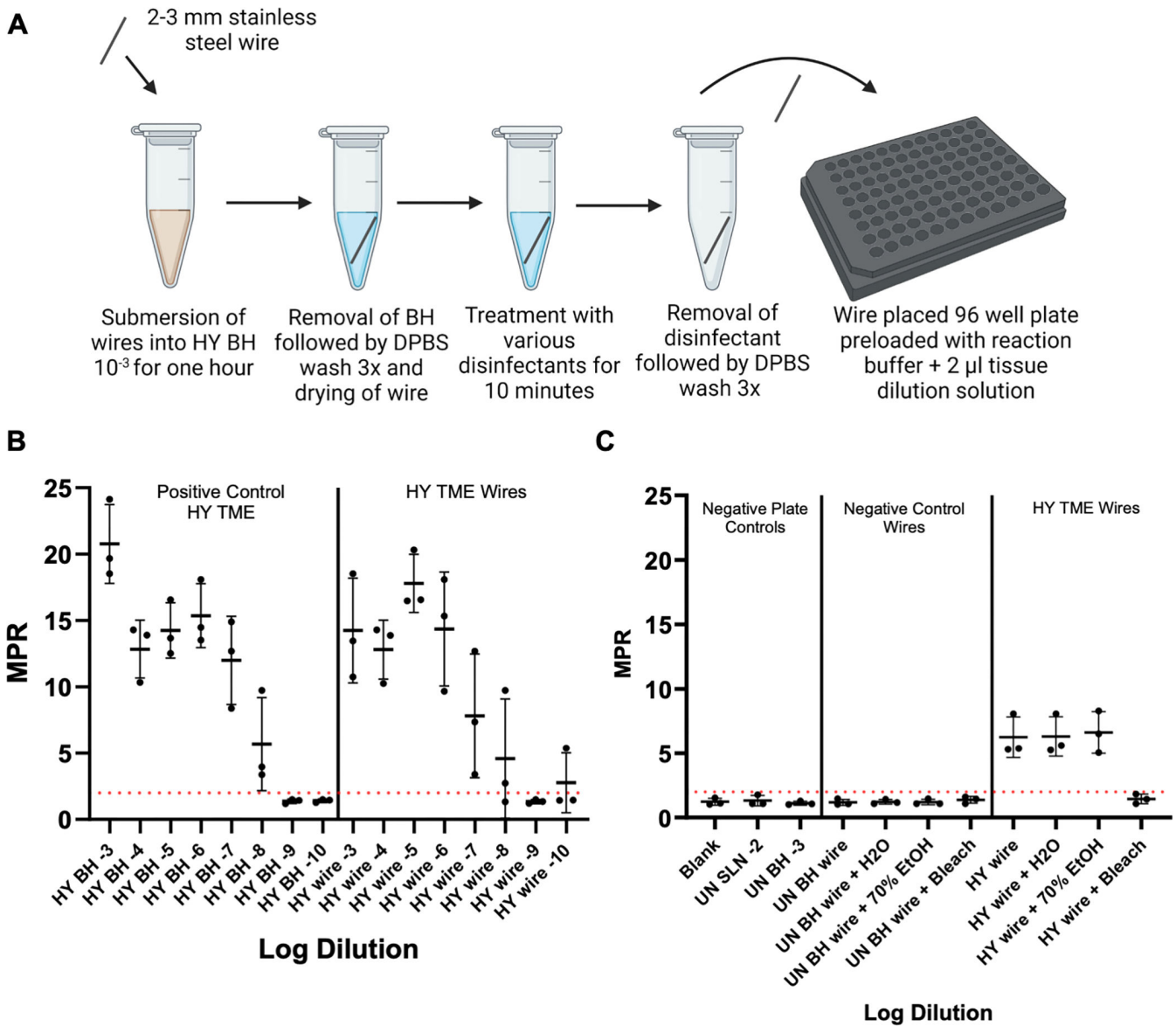
FIG 4 Direct surface measurement of prion seeding activity on stainless steel wire mirrors the results of surface-recovered prion seeding activity. (A)Overview of wire contamination and analysis by RT-QuIC (created with BioRender.com). (B)RT-QuIC detection of HY BH dilutions and stainless steel wires contaminated with HY BH dilutions. (C)RT-QuIC detection of contaminated stainless steel wires. A positive fluorescence threshold (illustrated by red line) was determined to be at 2. The maxpoint ratio reported is the ratio of the maximum fluorescence to the initial fluorescence reading obtained by the plate reader. Each point represents the average MPR from one biological replicate (mean ± standard deviation). For treated HY TME wires, each point is an average of 16 replicate wires, except one biological replicate for 70% EtOH-treated wires contained 15 replicate wires, and one biological replicate of H_2O-treated wires contained 14 replicate wires.

surfaces treated with bleach resulted in none ($n = 5$) of the animals developing clinical signs of prion disease at 300 dpi when the experiment was terminated (Fig. 5, panel D). Western blot analysis for the presence of PrP^{Sc} from these animals was consistent with the clinical diagnosis of disease (Fig. 5, panel E). Overall, the results from RT-QuIC and animal bioassay were congruent (Table 3).

The effect of environmental factors on RT-QuIC reactions

Given the wide-ranging use and degree of cleanliness of relevant clinical and laboratory surfaces, various concentrations of three distinct soil minerals [non-expanding kaolinite (Kao), expanding montmorillonite, and hectorite] were added to the tissue dilution
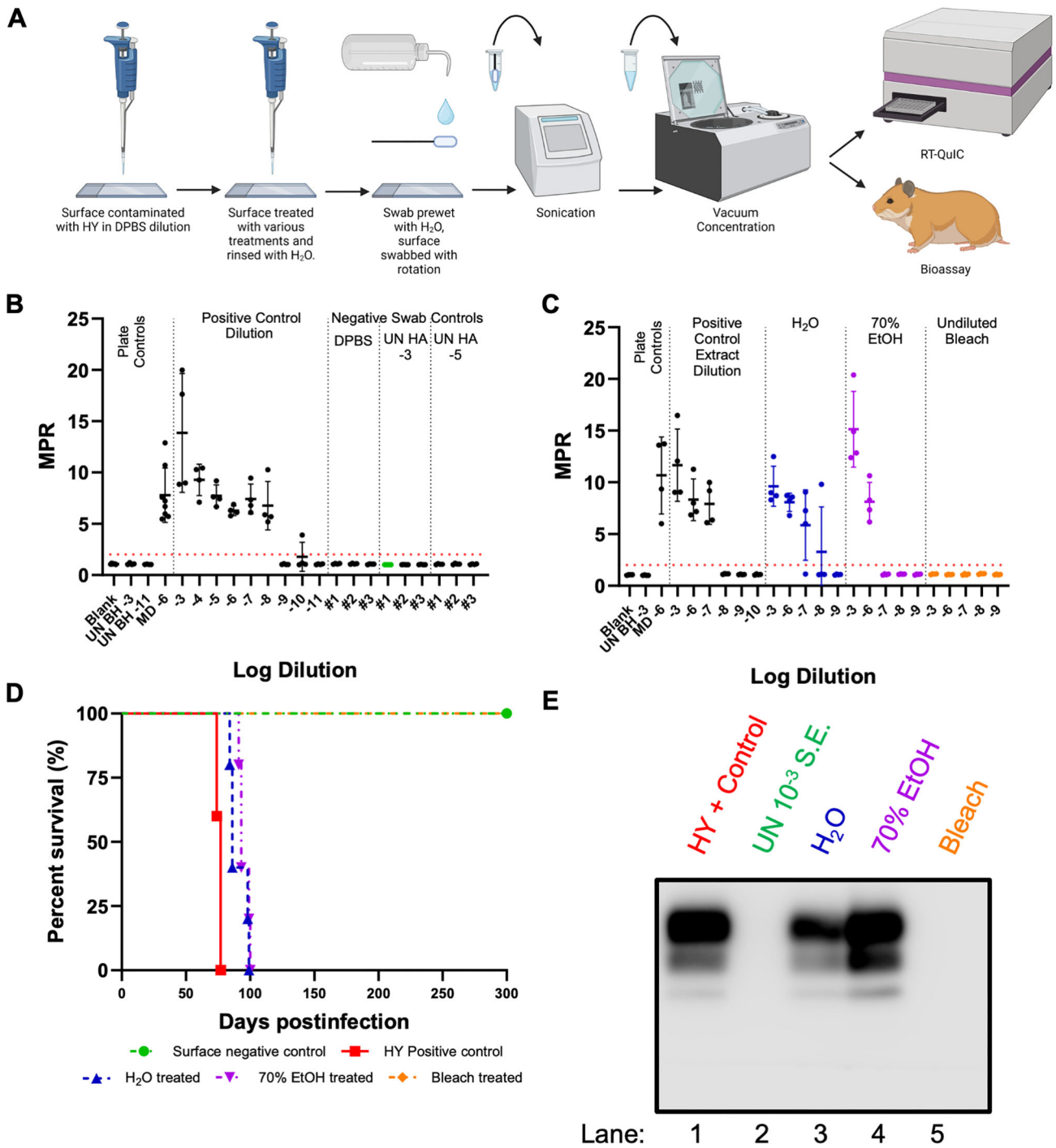
FIG 5 RT-QuIC and animal bioassay of swab extracts produced similar results. (A)Overview of surface prion contamination and swabbing procedure resulting in swab extracts that were analyzed by either (B and C)RT-QuIC (created with BioRender.com) (D)or animal bioassay. A positive fluorescence threshold (illustrated by the red line) was determined to be at 2. The maxpoint ratio reported is the ratio of the maximum fluorescence to the initial fluorescence reading obtained by the plate reader (mean ± standard deviation). (E)Western blot analysis of PK digested brain homogenates from bioassay results from panel D.

solution used for the preparation of UN HA BH negative plate controls and HY TME dilution series to investigate their potential impacts on the RT-QuIC reaction. Each of the aforementioned soil types was added to the tissue dilution solution at concentrations of 100, 10, 1, and 0.1 mg/mL, and this tissue dilution solution was used for the preparation of UN HA BH and HY TME dilution series (Fig. 6, panel A). The addition of the highest

TABLE 3 Comparison of RT-QuIC and bioassay results of treated prion-contaminated glass slide surfaces

	RT-QuIC SD$_{50}$/g of brain homogenate	RT-QuIC positive wells (10^{-3})	Incubation period (days)^a	Attack rate	PrP^{Sc} present on western blot
UN HA BH swab extract negative control	MPR< 2	0/4	>300	0/5	0/5
HY TME 10^{-4} positive control	11.37	4/4	76 ± 3	5/5	5/5
H$_2$O-treated swab extract	10.20	4/4	91 ± 7	5/5	5/5
70% ethanol-treated swab extract	9.20	4/4	95 ± 4	5/5	5/5
Bleach-treated swab extract	MPR< 2	0/4	>300	0/5	0/5

^{a}Average ± SD.

concentration of Kao led to a complete inhibition of the detection of the HY TME dilution series, yielding no fluorescence above the set positive fluorescence threshold of 2 (Fig. 6, panel B). Interestingly, the fluorescence curves of the uninfected BH dilutions with 100 mg/mL of Kao added showed distinct tracings (although below the positive threshold) when compared to the same dilutions without soil added (Fig. S7, panel A). The addition of 10, 1, and 0.1 mg/mL did not significantly ($P < 0.05$) alter the SD$_{50}$ of the HY dilution series compared to a no soil control (Fig. 5, panels C, D, and E). For hectorite, the addition of 10 mg/mL completely inhibited the RT-QuIC reaction, while the addition of 1 and 0.1 mg/mL did not significantly ($P < 0.05$) affect the SD$_{50}$ value sensitivity (Table 4). For montmorillonite (Mte), again the addition of 10 mg/mL of soil inhibited the RT-QuIC reaction. While 0.1 mg/mL of Mte had no significant ($P > 0.05$) effect on the sensitivity of the RT-QuIC reaction, the addition of 1 mg/mL led to an approximate 1 log increase in SD$_{50}$, which was statistically ($P < 0.05$) significant. In addition, 0.1 mg/mL Mte led to a decrease in the maximum fluorescence observed in each replicate well (Fig. S7, panel B). Of note, when performing experiments on factory new benchtop surfaces, an altered background fluorescence curve was observed, extending above the positive fluorescence threshold (Fig. S7, panel C), which was eliminated by washing with water (Fig. S7, panel C). Due to these findings, the impact of environmental contaminants such as dust and byproducts of manufacturing on RT-QuIC should be considered.

The addition of nanoparticles to RT-QuIC can increase the sensitivity of surface-recovered prions

The ability of silica nanoparticles to increase the sensitivity of RT-QuIC on surface-recovered HY prions was investigated. Stainless steel tokens were contaminated with 10^{-1} to 10^{-9} 10-fold serial dilutions of HY TME-infected brain homogenate in DPBS (mother dilutions), and contaminated surfaces were allowed to dry for 24 hours prior to swabbing, extraction, and RT-QuIC analysis as previously described. While low dilutions of brain homogenate are not generally tested due to the inhibitory effects on RT-QuIC, the addition of silica nanoparticles has previously been shown to overcome this inhibition (98). For this reason, a dilution series of 10^{-2} to 10^{-10} was investigated using both standard RT-QuIC and nanoparticle RT-QuIC (Nano-QuIC). Negative plate controls for standard RT-QuIC failed to yield MPR above the determined positive threshold of 2 (Fig. 7). One out of three replicates yielded positive signals in the negative plate controls for nanoparticle RT-QuIC reactions. When comparing standard RT-QuIC to nanoparticle RT-QuIC, a restoration of seeding was observed for the HY dilution 10^{-2} following the addition of nanoparticles, thus increasing the sensitivity of surface recovered HY prions by one order of magnitude.

DISCUSSION

The surface swab prion detection method effectively assessed the decontamination efficacy of two common disinfectants. Building upon our previous work indicating that prions can be recovered from surfaces with swabbing, here we show efficient recovery of prions from laboratory and clinically relevant surfaces (Fig. 1) (97). To investigate the utility of this methodology in assessing the effectiveness of prion decontamination
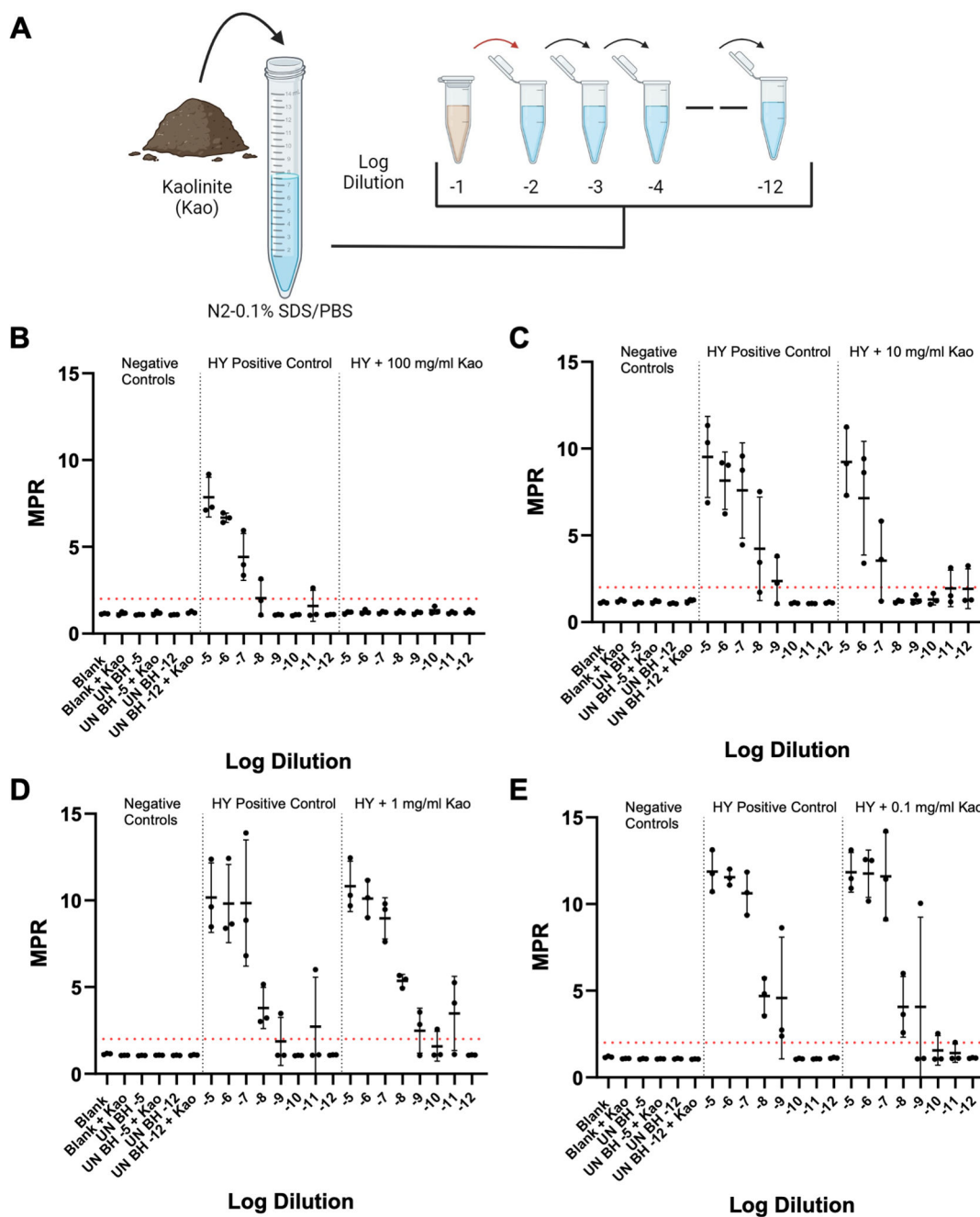
FIG 6 Impact of soil on RT-QuIC detection of HY dilutions is dependent on soil concentration. (A)Overview of soil spiking procedure of tissue dilution solution for RT-QuIC analysis (created with BioRender.com). (B)RT-QuIC detection of HY dilutions prepared in tissue dilution solution with 100mg/mL of kaolinite. (C)RT-QuIC detection of HY dilutions prepared in tissue dilution solution with 10mg/mL of Kao. (D)RT-QuIC detection of HY dilutions prepared in tissue dilution solution with 1mg/mL of Kao. (E)RT-QuIC detection of HY dilutions prepared in tissue dilution solution with 0.1mg/mL of Kao. Negative plate controls include blank and uninfected brain homogenate of 10^{-5} and 10^{-12} with and without soil. A positive plate control consisted of a HY dilution series prepared in standard tissue dilution solution. A positive fluorescence threshold (illustrated by red line) was determined to be at 2. The maxpoint ratio reported is the ratio of the maximum fluorescence to the initial fluorescence reading obtained by the plate reader. Each point represents the average MPR from one biological replicate (mean ± standard deviation).

procedures, we treated surfaces with either water as a negative decontamination control, 70% EtOH as an example of a common laboratory disinfectant, and sodium hypochlorite as a positive control for prion decontamination. We observed that 70% EtOH treatment of HY TME-contaminated surfaces resulted in the detection of RT-QuIC seeding activity in

TABLE 4 Comparison of log SD_{50}/g of brain homogenate, determined by RT-QuIC end-point dilutions, of the effects of soil on HY dilution seeding capabilities

Mineral	Soil concn (mg/mL)	HY	1	2	3	Avg± SD
Kaolinite		HY without soil	9.93	10.03	10.90	10.29 ± 0.44
	100	HY with soil	MPR< 2	MPR< 2	MPR< 2	MPR< 2
		HY without soil	10.20	11.70	10.93	10.94 ± 0.61
	10	HY with soil	8.37	10.31	9.96	9.55 ± 0.84
		HY without soil	10.70	12.25	10.37	11.11 ± 0.82
	1	HY with soil	11.52	12.25	10.70	11.49 ± 0.63
		HY without soil	10.70	10.93	10.93	10.85 ± 0.11
	0.1	HY with soil	11.82	10.37	11.31	11.17 ± 0.60
Montmorillonite		HY without soil	10.70	10.03	10.20	10.31 ± 0.28
	10	HY with soil	MPR< 2	MPR< 2	MPR< 2	MPR< 2
		HY without soil	10.20	12.08	10.47	10.92 ± 0.83
	1	HY with soil	11.70	11.70	12.14	11.85 ± 0.21[a]
		HY without soil	10.47	11.03	10.03	10.51 ± 0.41
	0.1	HY with soil	11.70	11.47	10.20	11.12 ± 0.66
Hectorite		HY without soil	9.92	10.37	9.37	9.89 ± 0.41
	10	HY with soil	MPR< 2	MPR< 2	MPR< 2	MPR< 2
		HY without soil	9.37	10.03	10.46	9.95 ± 0.45
	1	HY with soil	9.93	10.20	11.03	10.39 ± 0.47
		HY without soil	10.47	10.03	10.70	10.40 ± 0.28
	0.1	HY with soil	10.20	10.70	11.44	10.78 ± 0.51

[a]$p<0.05$.

the swab extracts with a similar SD_{50} compared to swab extracts from water-treated HY TME-contaminated surfaces (Fig. 3) consistent with previous studies suggesting the ineffectiveness of ethanol as a prion disinfectant (39, 42, 99, 100). Consistent with previous findings, RT-QuIC testing of swab extracts from bleach-treated surfaces failed to detect prion RT-QuIC seeding activity (Fig. 3) (58, 86, 89, 101). Importantly, control experiments determined that the failure to detect prions on bleach-treated surfaces was not due to residual bleach in the surface swab extract inhibiting the RT-QuIC reaction but was instead due to the destruction of prions (Fig. 2).

The reduction in RT-QuIC seeding activity of surface swab extracts corresponded with a reduction in the seeding activity of prion-coated stainless steel wires. To investigate the possibility that the reduction in RT-QuIC seeding activity of the surface swab extracts is due to a failure to recover infectious prions from the surface, we coated stainless steel wires with HY TME brain homogenate and placed them directly into RT-QuIC reaction tubes to test for prions bound to the surface (58). As a positive control, stainless steel wires were coated with a 10-fold dilution series of HY TME-infected brain homogenate and placed directly into the RT-QuIC reactions, resulting in a similar sensitivity for prion detection as HY TME homogenate directly added to the RT-QuIC reaction (Fig. 4, panel B). Treatment of the HY TME-contaminated stainless steel wires with either water or 70% EtOH resulted in similar RT-QuIC seeding activity consistent with a lack of prion inactivation observed in the surface swab extracts (Fig. 4, panel C). Treatment of the HY TME-contaminated prion wires with bleach resulted in a failure to detect RT-QuIC seeding activity on the wire surface (Fig. 4, panel C) similar to previous studies (58, 86). The combination of the failure to detect RT-QuIC seeding activity from surface swab extracts and bleach-treated stainless steel wires indicates that the surface swab extract findings are predictive of the prion contamination status of the surface tested.

The RT-QuIC seeding activity and prion infectivity of surface swab extracts are congruent. To investigate the possibility that RT-QuIC seeding activity may not correspond with prion infectivity, we designed an experiment where the same surface extracts were tested for seeding activity using RT-QuIC and i.c. inoculated into hamsters
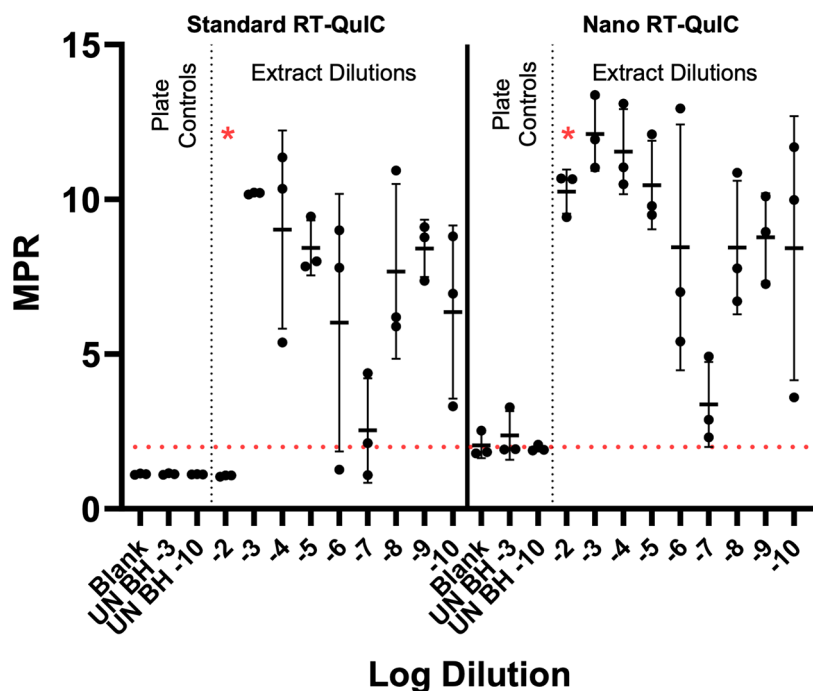
FIG 7 Nano RT-QuIC increases the sensitivity of RT-QuIC detection of surface-recovered HY. RT-QuIC and nano RT-QuIC detection of stainless steel surface-recovered HY dilutions from vertical dilution experiment. Negative plate controls include blank and uninfected brain homogenate dilution of 10^{-3} and 10^{-10}. A positive fluorescence threshold (illustrated by the red line) was determined to be at an MPR of 2. The maxpoint ratio reported is the ratio of the maximum fluorescence to the initial fluorescence reading obtained by the plate reader. Each point represents the average MPR from one technical replicate (mean ± standard deviation).

to examine for prion infectivity. We found that surfaces treated with either water or 70% EtOH contained RT-QuIC seeding activity, which also resulted in all the animals in each group developing prion disease (Fig. 5). Interestingly, the seeding activity SD_{50} and incubation period in hamsters were similar between the water- and 70% EtOH-treated surface swab extracts, suggesting that both methods produced qualitatively similar results (Fig. 5) (102). The bleach-treated surface swab extracts failed to result in RT-QuIC seeding activity and did not result in clinical signs of prion disease in hamsters or evidence of a subclinical infection, at 300 days post-infection (Fig. 5). As 300 days post-infection is a longer incubation period than a single i.c. LD_{50} of HY TME, we interpret this finding that bleach treatment completely inactivated HY TME infectivity (103, 104). As we applied $5 \times 10^{5.8}$ i.c. LD_{50} of prion infectivity to the surface, we interpret this negative result as a >5-log reduction in prion infectivity. Overall, under the conditions tested, we found that RT-QuIC seeding activity and animal bioassay produced similar results.

Nano-QuIC may enhance the sensitivity of prion detection from surface swab extracts. A weakness of the current study is that the swab extract must be diluted 100-fold prior to RT-QuIC analysis, as higher concentrations (i.e., lower dilutions) of swab extract inhibit the detection of PrP^{Sc} in RT-QuIC (Fig. 7). This inhibitory phenomenon has previously been observed with low dilution of tissue homogenates (102, 105–107). A recently described modification of RT-QuIC that includes nanoparticles (nano-QuIC) may overcome this limitation (98). Here, we found that the use of nano RT-QuIC resulted in the reliable detection of prions in 10-fold swab extract dilutions, effectively increasing the sensitivity of the assay by an order of magnitude (Fig. 7). While promising, the effectiveness of Nano-QuIC to overcome RT-QuIC inhibitors may differ with the nature of

the contents of the extract or the prion strain tested. Further studies are warranted to evaluate the effectiveness of nano RT-QuIC for surface swab extract detection of prions.

Testing surfaces for residual prion infectivity can be integrated into a comprehensive prion safety program. A recent report provided a methodology to test surfaces and tools to verify that prion decontamination was effective (96). Here, we extended this important work by integrating surface swabbing that may prove to be useful where the application of media for direct testing by RT-QuIC is impractical. In laboratory settings, this can be used to verify that laboratory space is decontaminated and to evaluate the potential for cross-contamination from disinfected necropsy tools used between animals and/or tissues. Similarly, in clinical settings, surfaces and instruments can be tested for the presence of residual prions to reduce the risk of iatrogenic transmission. Here, we show the limitations of the technique as the addition of soil and residues from the manufacturing process of laboratory benchtop can adversely affect RT-QuIC results (Fig. 6; Fig. S7; Table 4). From a practical perspective, laboratory and clinical surfaces should be as free of dust and chemicals prior to surveying for prion seeding activity. Anomalous RT-QuIC results from surfaces not described here should be interpreted with caution. Additional analysis or experimentation to discriminate between bona fide seeding activity and environmental artifact would be justified. Finally, the methodologies described here can be adapted for prion and prion-like diseases that support detection using RT-QuIC (92–94, 96, 108, 109).

MATERIALS AND METHODS

Prion sources

Brain tissue was collected from hamsters infected with hyper transmissible mink encephalopathy at the terminal stage of disease containing $10^{9.3}$ i.c. LD_{50}/g of prion infectivity as previously described (104). Brain tissue was homogenized in Dulbecco's phosphate-buffered saline (Mediatech, Herndon, VA, USA) to 10%, wt/vol using syringe and needle homogenization. The 10%, wt/vol HY BH aliquots were clarified by centrifugation at 450 g for 30 seconds. Supernatants were transferred into new 1.5 mL microcentrifuge tubes and stored at −80°C.

Surface contamination—vertical dilution experiments

Ten percent uninfected brain homogenate (BH) was used to prepare serial 10-fold dilutions in DPBS (10^{-2}–10^{-9}) for use as negative controls. The dilutions applied directly to the surface will be referred to as mother dilutions. Ten percent HY BH was used to prepare serial 10-fold mother dilutions in DPBS (10^{-2}–10^{-9}). Fifty microliters of each dilution in the series was applied in triplicate onto the surface of Sakura, Tissue-Tek SmartWrite Charge, white frosted glass slides (product number: 9036), stainless steel tokens (Lindstrom Grade 304, Part# FW5X01000, Lot# W033000812), or laboratory benchtop surfaces (Kewaunee, Kemresin epoxy resin benchtop, 1″ cubes with one finished surface). Mother dilutions were stored at −80°C for further use in RT-QuIC plates. Glass slide surfaces were partitioned using a hydrophobic marker to prevent the runoff water generated during rinsing from reaching other prion-contaminated areas. Negative controls applied to all surface materials included DPBS, UN 10^{-2}, and UN 10^{-9}. Fifty microliters of each negative control was applied in triplicate. All surfaces were allowed to dry overnight.

Surface contamination—horizontal dilution experiment

HY 10% BH was used to prepare 10-fold serial dilutions in DPBS (10^{-2} and 10^{-4} were used for this experiment). UN 10% BH was used to prepare 10-fold serial dilutions in DPBS (10^{-2} and 10^{-4} were used for this experiment). Negative controls applied to all surfaces included DPBS, UN 10^{-2}, and UN 10^{-4} BH. Fifty microliters of each mother dilution was

applied in triplicate to each respective surface. The remaining mother dilutions were stored at −80°C. All surfaces were allowed to dry overnight.

Surface disinfection

For surface disinfection, either MQ H_2O, 70% EtOH, or undiluted bleach (Clorox, Sodium Hypochlorite 8.25%) was used as a treatment. Prior to 70% EtOH treatment, boxes were drawn around the prion-contaminated area on glass slide surfaces with a hydrophobic marker to prevent the dispersal of the treatment. Contaminated glass slide surfaces, stainless steel tokens, and benchtop surfaces were subjected to 70, 60, or 90 µL, respectively, of one of the three disinfection treatments at room temperature for 10 minutes. After 10 minutes, the treated surfaces were rinsed thoroughly with water prior to swabbing. Following rinsing, if the surfaces remained wet, foam swabs were not prewet prior to swabbing, if surfaces were dry, foam swabs were prewet. All treatments were performed in triplicate on separate prion-contaminated areas.

Surface swabbing, swab extraction, and concentration

Extracts from swabbed surfaces were performed as previously described (97). Briefly, foam swabs (Fisher brand, Catalog #14-960-3E) were prewet with MQ water. Each surface was swabbed with a separate, new swab approximately 10 times with rotation. Swab handles were cut to fit into microcentrifuge tubes preloaded with 250 µL DPBS, and swabs were immediately placed into designated tubes. The swabs, in microcentrifuge tubes, were sonicated (Q700 QSonica sonicator) for a total of 15 seconds (5 seconds of sonication and 5 seconds of rest) at an average of 80 watts. After sonication, swabs were briefly centrifuged (Thermo Scientific mini-centrifuge) prior to the transfer of the extract into a new tube. The swab extracts were then subjected to vacuum concentration (Thermo Scientific savant speedvac SPD1030) for a total of 2 hours at 45°C and a vacuum setting of 5.1. Pellets were resuspended with 50 µL of H_2O prior to RT-QuIC analysis.

Bleach RT-QuIC inhibition control experiment

Two groups of glass slides were contaminated with 10^{-2} HY as described above. One prion-contaminated surface was treated with undiluted bleach as described in Surface Disinfection section. The treated and rinsed surface was then swabbed as described above to capture any residual bleach from the surface. This same swab was then used to immediately swab the second 10^{-2} HY-contaminated surface. The swabs in microcentrifuge tubes were then subjected to the swab extraction and concentration protocol described below.

Dilution preparation for RT-QuIC

For the vertical dilution experiment, each swab extract in a dilution series was 10-fold diluted into N2-0.1% SDS/PBS (N-2 supplement (100×); ThermoFisher catalog #17502048). Positive plate control dilutions for vertical dilution experiments included the original mother dilution series diluted 10-fold into N2-0.1%SDS/PBS (Fig. S1). HY was diluted 10-fold into N2-0.1%SDS/PBS for use as a positive control in swab control plates. For the horizontal dilution experiment, both untreated and treated 10^{-2} swab extracts were subjected to further 10-fold serial dilution in N2-0.1%SDS/PBS (10^{-3}–10^{-9}). The untreated swab extracts were used as a positive plate control.

RT-QuIC reaction

RT-QuIC was performed as previously described (97). Briefly, negative plate controls included a blank sample (N2-0.1%SDS/PBS) and the lowest dilution included in the plate of UN BH. The reaction buffer was prepared to the following concentrations: 1× PBS, 170 mM, 1 mM EDTA, 10 µM ThT, and 0.1 mg/mL of recombinant hamster prion protein (recHaPrP; Priogen Corp, St. Paul, MN, USA). Two microliters of each sample was added to

98 µL of the reaction buffer. Cycle duration was 45 minutes, and fluorescence readings were recorded once per cycle for a total of 65 cycles. RT-QuIC reactions were performed in a BMG FLUOstar Omega plate reader (BMG Labtech, Cary, NC, USA). Shaking at 700 rpm double orbital with alternating cycles of 1 minute of shaking followed by 1 minute of rest. The MPR was obtained by dividing the maximum fluorescence reading in each well by the initial (background) fluorescence. A positive fluorescence threshold was established at 2. A cutoff of 45 cycles (33 hours) was established for positive time to fluorescence following the *post hoc* analysis of the time to fluorescence for negative and positive controls from 84 plates. SD_{50} determinations (dilution at which 50% of replicate wells give off fluorescence above the defined positive threshold) were calculated using the method of Reed and Muench (110)

Nano-QuIC reaction comparison

For Nano-QuIC, experiments were performed as previously described (98). Briefly, RT-QuIC reaction plates were performed with standard RT-QuIC and Nano-QuIC ran in parallel. The Nano-QuIC reaction buffer was prepared to the following concentrations: 1× PBS, 300 mM NaCl, 500 µM EDTA, 50 µM ThT, 2.5 mg/mL 50 nm silica nanoparticles, and 0.1 mg/mL of recombinant hamster prion protein. Negative plate controls included tissue dilution solution, UN HA BH 10^{-3} and UN HA BH 10^{-10}. All test samples were investigated with standard reaction buffer and Nano-QuIC reaction buffer within the same plate. RT-QuIC was performed as previously described.

Wire-QuIC reaction

Wire-QuIC reactions were performed as previously described (58). Briefly, 2–3 mm stainless steel wires were incubated with 50 µL of HY BH 10^{-3}, prepared in DPBS, following a brief vortex in microcentrifuge tubes for 1 hour. Following incubation, BH was discarded, and wires were washed with DPBS three times. Wires in microcentrifuge tubes were allowed to dry overnight. For each treatment group, 16 wires were used. A volume of 50 µL of each disinfectant was added to the wires for 10 minutes followed by thorough rinsing. Negative plate controls included a blank sample, UN SLN 10^{-2}, and UN HA BH 10^{-3}. Negative wire controls included wires incubated with UN HA BH 10^{-3} that underwent either no treatment, treatment with H_2O, treatment with 70% EtOH, or treatment with undiluted bleach. One wire was added to each well. Each well contained 98 µL of reaction buffer and 2 µL of tissue dilution solution. RT-QuIC was performed as previously described.

Effects of soil on RT-QuIC seeding capabilities experiment

Briefly, a stock of tissue dilution solution was created for each soil mineral and each soil final concentration. These included kaolinite (100, 10, 1, and 0.1 mg/mL), montmorillonite (10, 1, and 0.1 mg/mL), and hectorite (10, 1, and 0.1 mg/mL). Stocks were generated by adding the appropriate amount of soil to N2-0.1% SDS/PBS followed by vortexing to achieve thorough mixing. A 10-fold dilution series was generated for HY TME BH and UN HA BH in standard N2-0.1%SDS/PBS and soil N2-0.1%SDS/PBS. RT-QuIC was performed as previously described. Negative plate controls included a blank sample (without soil), UN HA BH 10^{-5} (without soil), and UN HA BH 10^{-12} (without soil). Negative soil controls included a blank (with soil added), UN HA BH 10^{-5} (with soil added), and UN HA BH 10^{-12} (with soil added).

Bioassay

Male 3–4-week-old Syrian hamsters were intracerebrally inoculated with 20 µL of either a 1:10 dilution of swab extracts or a HY 10^{-4} BH dilution. The animals were monitored three times a week for the onset of neurological signs, and the incubation period was

calculated as the difference in days between the date of inoculation and the onset of clinical signs of prion infection.

AUTHOR AFFILIATIONS

[1]Department of Medical Microbiology and Immunology, School of Medicine, Creighton University, Omaha, Nebraska, USA

[2]College of Saint Mary's, Omaha, Nebraska, USA

[3]Biostatistical Core Facility, Creighton University, Omaha, Nebraska, USA

[4]Department of Veterinary and Biomedical Sciences, College of Veterinary Medicine, University of Minnesota, St. Paul, Minnesota, USA

[5]Minnesota Center for Prion Research and Outreach, College of Veterinary Medicine, University of Minnesota, St. Paul, Minnesota, USA

[6]Department of Veterinary Population Medicine, College of Veterinary Medicine, University of Minnesota, St. Paul, Minnesota, USA

[7]Prion Research Center, Colorado State University, Fort Collins, Colorado, USA

AUTHOR ORCIDs

Marc D. Schwabenlander http://orcid.org/0000-0001-9664-6890
Jason C. Bartz http://orcid.org/0000-0003-4081-7886

AUTHOR CONTRIBUTIONS

Sara M. Simmons, Conceptualization, Data curation, Formal analysis, Investigation, Methodology, Writing – original draft, Writing – review and editing | Vivianne L. Payne, Data curation, Investigation, Writing – review and editing | Jay G. Hrdlicka, Data curation, Investigation, Writing – review and editing | Jack Taylor, Data curation, Formal analysis, Writing – review and editing | Peter A. Larsen, Methodology, Writing – review and editing | Tiffany M. Wolf, Methodology, Writing – review and editing | Marc D. Schwabenlander, Methodology, Writing – review and editing | Qi Yuan, Conceptualization, Formal analysis, Funding acquisition, Writing – review and editing | Jason C. Bartz, Conceptualization, Funding acquisition, Project administration, Supervision, Writing – original draft, Writing – review and editing

ETHICS APPROVAL

All procedures involving animals were approved and in compliance with the Guide for the Care and Use of Laboratory Animals by the Creighton University Institutional Animal Care and Use Committee.

ADDITIONAL FILES

The following material is available online.

Supplemental Material

Figure S1 (mSphere00504-24-s0001.tiff). Dilution preparation.

Figure S2 (mSphere00504-24-s0002.tiff). Bleach is an effective disinfectant for HY contaminated stainless steel surfaces.

Figure S3 (mSphere00504-24-s0003.tiff). Bleach is an effective disinfectant for HY contaminated benchtop surfaces.

Figure S4 (mSphere00504-24-s0004.tiff). Bleach is an effective disinfectant for HY contaminated glass surfaces.

Figure S5 (mSphere00504-24-s0005.tiff). Impact of montmorillonite on RT-QuIC detection of HY dilutions is dose dependent.

Figure S6 (mSphere00504-24-s0006.tiff). Impact of Hectorite on RT-QuIC detection of HY dilutions is dose dependent.

Figure S7 (mSphere00504-24-s0007.tiff). Addition of environmental contamination impacts RT-QuIC.

Legends (mSphere00504-24-s0008.docx). Supplemental figure legends.

REFERENCES

1. Gajdusek DC, Zigas V. 1957. Degenerative disease of the central nervous system in New Guinea; the endemic occurrence of kuru in the native population. N Engl J Med 257:974–978. https://doi.org/10.1056/NEJM195711142572005

2. Lugaresi E, Medori R, Montagna P, Baruzzi A, Cortelli P, Lugaresi A, Tinuper P, Zucconi M, Gambetti P. 1986. Fatal familial insomnia and dysautonomia with selective degeneration of thalamic nuclei. N Engl J Med 315:997–1003. https://doi.org/10.1056/NEJM198610163151605

3. Masters CL, Gajdusek DC, Gibbs CJ. 1981. Creutzfeldt-Jakob disease virus isolations from the Gerstmann-Sträussler syndrome. Brain 104:559–588. https://doi.org/10.1093/brain/104.3.559

4. Gibbs CJ, Gajdusek DC, Asher DM, Alpers MP, Beck E, Daniel PM, Matthews WB. 1968. Creutzfeldt-Jakob disease (spongiform encephalopathy): transmission to the chimpanzee. Science 161:388–389. https://doi.org/10.1126/science.161.3839.388

5. Babelhadj B, Di Bari MA, Pirisinu L, Chiappini B, Gaouar SBS, Riccardi G, Marcon S, Agrimi U, Nonno R, Vaccari G. 2018. Prion disease in dromedary camels, Algeria. Emerg Infect Dis 24:1029–1036. https://doi.org/10.3201/eid2406.172007

6. Wells GAH, Scott AC, Johnson CT, Gunning RF, Hancock RD, Jeffrey M, Dawson M, Bradley R. 1987. A novel progressive spongiform encephalopathy in cattle. Vet Rec 121:419–420. https://doi.org/10.1136/vr.121.18.419

7. Williams ES, Young S. 1982. Spongiform encephalopathy of Rocky Mountain elk. J Wildl Dis 18:465–471. https://doi.org/10.7589/0090-3558-18.4.465

8. Williams ES, Young S. 1980. Chronic wasting disease of captive mule deer: a spongiform encephalopathy. J Wildl Dis 16:89–98. https://doi.org/10.7589/0090-3558-16.1.89

9. Stamp JT, Brotherston JG, Zlotnik I, Mackay JM, Smith W. 1959. Further studies on scrapie. J Comp Pathol 69:268–280. https://doi.org/10.1016/s0368-1742(59)80026-6

10. Prusiner SB. 1982. Novel proteinaceous infectious particles cause scrapie. Science 216:136–144. https://doi.org/10.1126/science.6801762

11. Bolton DC, McKinley MP, Prusiner SB. 1982. Identification of a protein that purifies with the scrapie prion. Science 218:1309–1311. https://doi.org/10.1126/science.6815801

12. Oesch B, Westaway D, Wälchli M, McKinley MP, Kent SBH, Aebersold R, Barry RA, Tempst P, Teplow DB, Hood LE, Prusiner SB, Weissmann C. 1985. A cellular gene encodes scrapie PrP 27-30 protein. Cell 40:735–746. https://doi.org/10.1016/0092-8674(85)90333-2

13. Caughey B, Raymond GJ. 1991. The scrapie-associated form of PrP is made from a cell surface precursor that is both protease- and phospholipase-sensitive. J Biol Chem 266:18217–18223. https://doi.org/10.1016/S0021-9258(18)55257-1

14. Deleault NR, Harris BT, Rees JR, Supattapone S. 2007. Formation of native prions from minimal components *in vitro*. Proc Natl Acad Sci U S A. 104:9741–9746. https://doi.org/10.1073/pnas.0702662104

15. Wang F, Wang X, Yuan CG, Ma J. 2010. Generating a prion with bacterially expressed recombinant prion protein. Science 327:1132–1135. https://doi.org/10.1126/science.1183748

16. Come JH, Fraser PE, Lansbury PT. 1993. A kinetic model for amyloid formation in the prion diseases: importance of seeding. Proc Natl Acad Sci U S A 90:5959–5963. https://doi.org/10.1073/pnas.90.13.5959

17. Frontzek K, Bardelli M, Senatore A, Henzi A, Reimann RR, Bedir S, Marino M, Hussain R, Jurt S, Meisl G, Pedotti M, Mazzola F, Siligardi G, Zerbe O, Losa M, Knowles T, Lakkaraju A, Zhu C, Schwarz P, Hornemann S, Holt MG, Simonelli L, Varani L, Aguzzi A. 2022. A conformational switch controlling the toxicity of the prion protein. Nat Struct Mol Biol 29:831–840. https://doi.org/10.1038/s41594-022-00814-7

18. Lakkaraju AKK, Frontzek K, Lemes E, Herrmann U, Losa M, Marpakwar R, Aguzzi A. 2021. Loss of PIKfyve drives the spongiform degeneration in prion diseases. EMBO Mol Med 13:e14714. https://doi.org/10.15252/emmm.202114714

19. Brandner S, Isenmann S, Raeber A, Fischer M, Sailer A, Kobayashi Y, Marino S, Weissmann C, Aguzzi A. 1996. Normal host prion protein necessary for scrapie-induced neurotoxicity. Nature 379:339–343. https://doi.org/10.1038/379339a0

20. Chiesa R, Drisaldi B, Quaglio E, Migheli A, Piccardo P, Ghetti B, Harris DA. 2000. Accumulation of protease-resistant prion protein (PrP) and apoptosis of cerebellar granule cells in transgenic mice expressing a PrP insertional mutation. Proc Natl Acad Sci U S A 97:5574–5579. https://doi.org/10.1073/pnas.97.10.5574

21. Fraser H, Dickinson AG. 1968. The sequential development of the brain lesions of scrapie in three strains of mice. J Comp Pathol 78:301–311. https://doi.org/10.1016/0021-9975(68)90006-6

22. Bartz JC. 2016. Prion strain diversity. Cold Spring Harb Perspect Med 6:a024349. https://doi.org/10.1101/cshperspect.a024349

23. Bessen RA, Marsh RF. 1994. Distinct PrP properties suggest the molecular basis of strain variation in transmissible mink encephalopathy. J Virol 68:7859–7868. https://doi.org/10.1128/jvi.68.12.7859-7868.1994

24. Prusiner SB. 2012. A unifying role for prions in neurodegenerative diseases. Science 336:1511–1513. https://doi.org/10.1126/science.1222951

25. Meyer-Luehmann M, Coomaraswamy J, Bolmont T, Kaeser S, Schaefer C, Kilger E, Neuenschwander A, Abramowski D, Frey P, Jaton AL, Vigouret JM, Paganetti P, Walsh DM, Mathews PM, Ghiso J, Staufenbiel M, Walker LC, Jucker M. 2006. Exogenous induction of cerebral β-amyloidogenesis is governed by agent and host. Science 313:1781–1784. https://doi.org/10.1126/science.1131864

26. Jucker M, Walker LC. 2013. Self-propagation of pathogenic protein aggregates in neurodegenerative diseases. Nature 501:45–51. https://doi.org/10.1038/nature12481

27. Eisele YS, Obermüller U, Heilbronner G, Baumann F, Kaeser SA, Wolburg H, Walker LC, Staufenbiel M, Heikenwalder M, Jucker M. 2010.

Peripherally applied Aβ-containing inoculates induce cerebral beta-amyloidosis. Science 330:980–982. https://doi.org/10.1126/science.1194516

28. Walker LC, Lynn DG, Chernoff YO. 2018. A standard model of Alzheimer's disease? Prion 12:261–265. https://doi.org/10.1080/19336896.2018.1525256

29. Walker LC. 2018. Prion-like mechanisms in Alzheimer disease. Handb Clin Neurol 153:303–319. https://doi.org/10.1016/B978-0-444-63945-5.00016-7

30. Rasmussen J, Mahler J, Beschorner N, Kaeser SA, Häsler LM, Baumann F, Nyström S, Portelius E, Blennow K, Lashley T, Fox NC, Sepulveda-Falla D, Glatzel M, Oblak AL, Ghetti B, Nilsson KPR, Hammarström P, Staufenbiel M, Walker LC, Jucker M. 2017. Amyloid polymorphisms constitute distinct clouds of conformational variants in different etiological subtypes of Alzheimer's disease. Proc Natl Acad Sci U S A 114:13018–13023. https://doi.org/10.1073/pnas.1713215114

31. Just MK, Gram H, Theologidis V, Jensen PH, Nilsson KPR, Lindgren M, Knudsen K, Borghammer P, Van Den Berge N. 2022. Alpha-synuclein strain variability in body-first and brain-first synucleinopathies. Front Aging Neurosci 14:907293. https://doi.org/10.3389/fnagi.2022.907293

32. Lau A, So RWL, Lau HHC, Sang JC, Ruiz-Riquelme A, Fleck SC, Stuart E, Menon S, Visanji NP, Meisl G, Faidi R, Marano MM, Schmitt-Ulms C, Wang Z, Fraser PE, Tandon A, Hyman BT, Wille H, Ingelsson M, Klenerman D, Watts JC. 2020. α-synuclein strains target distinct brain regions and cell types. Nat Neurosci 23:21–31. https://doi.org/10.1038/s41593-019-0541-x

33. Ayers JI, Fromholt S, Koch M, DeBosier A, McMahon B, Xu G, Borchelt DR. 2014. Experimental transmissibility of mutant SOD1 motor neuron disease. Acta Neuropathol. 128:791–803. https://doi.org/10.1007/s00401-014-1342-7

34. Sacino AN, Brooks M, Thomas MA, McKinney AB, Lee S, Regenhardt RW, McGarvey NH, Ayers JI, Notterpek L, Borchelt DR, Golde TE, Giasson BI. 2014. Intramuscular injection of α-synuclein induces CNS α-synuclein pathology and a rapid-onset motor phenotype in transgenic mice. Proc Natl Acad Sci U S A 111:10732–10737. https://doi.org/10.1073/pnas.1321785111

35. Braak H, Del Tredici K, Rüb U, de Vos RAI, Jansen Steur ENH, Braak E. 2003. Staging of brain pathology related to sporadic Parkinson's disease. Neurobiol Aging 24:197–211. https://doi.org/10.1016/s0197-4580(02)00065-9

36. Banerjee G, Farmer SF, Hyare H, Jaunmuktane Z, Mead S, Ryan NS, Schott JM, Werring DJ, Rudge P, Collinge J. 2024. Iatrogenic Alzheimer's disease in recipients of cadaveric pituitary-derived growth hormone. Nat Med 30:394–402. https://doi.org/10.1038/s41591-023-02729-2

37. Singh CSB, Johns KM, Kari S, Munro L, Mathews A, Fenninger F, Pfeifer CG, Jefferies WA. 2024. Conclusive demonstration of iatrogenic Alzheimer's disease transmission in a model of stem cell transplantation. Stem Cell Rep 19:456–468. https://doi.org/10.1016/j.stemcr.2024.02.012

38. Alper T, Cramp WA, Haig DA, Clarke MC. 1967. Does the agent of scrapie replicate without nucleic acid? Nature 214:764–766. https://doi.org/10.1038/214764a0

39. Bernoulli C, Siegfried J, Baumgartner G, Regli F, Rabinowicz T, Gajdusek DC, Gibbs CJ. 1977. Danger of accidental person-to-person transmission of Creutzfeldt-Jakob disease by surgery. Lancet 1:478–479. https://doi.org/10.1016/s0140-6736(77)91958-4

40. Brown P, Rohwer RG, Green EM, Gajdusek DC. 1982. Effect of chemicals, heat, and histopathologic processing on high-infectivity hamster-adapted scrapie virus. J Infect Dis 145:683–687. https://doi.org/10.1093/infdis/145.2.683

41. Brown P, Gibbs CJ, Amyx HL, Kingsbury DT, Rohwer RG, Sulima MP, Gajdusek DC. 1982. Chemical disinfection of Creutzfeldt-Jakob disease virus. N Engl J Med 306:1279–1282. https://doi.org/10.1056/NEJM198205273062107

42. Dickinson AG, Taylor DM. 1978. Resistance of scrapie agent to decontamination. N Engl J Med 299:1413–1414. https://doi.org/10.1056/NEJM197812212992512

43. Fichet G, Comoy E, Dehen C, Challier L, Antloga K, Deslys J-P, McDonnell G. 2007. Investigations of a prion infectivity assay to evaluate methods of decontamination. J Microbiol Methods 70:511–518. https://doi.org/10.1016/j.mimet.2007.06.005

44. Fichet G, Antloga K, Comoy E, Deslys JP, McDonnell G. 2007. Prion inactivation using a new gaseous hydrogen peroxide sterilisation process. J Hosp Infect 67:278–286. https://doi.org/10.1016/j.jhin.2007.08.020

45. Hunter GD, Millson GC. 1964. Studies on the heat stability and chromatographic behavior of the scrapie agent. J Gen Microbiol 37:251–258. https://doi.org/10.1099/00221287-37-2-251

46. Pattison IH. 1965. Resistance of the scrapie agent to formalin. J Comp Pathol 75:159–164. https://doi.org/10.1016/0021-9975(65)90006-x

47. Fraser H, Farquhar CF, McConnell I, Davies D. 1989. The scrapie disease process is unaffected by ionising radiation. Prog Clin Biol Res 317:653–658.

48. Fraser H, Farquhar CF. 1987. Ionising radiation has no influence on scrapie incubation period in mice. Vet Microbiol 13:211–223. https://doi.org/10.1016/0378-1135(87)90084-8

49. Woerman AL, Kazmi SA, Patel S, Freyman Y, Oehler A, Aoyagi A, Mordes DA, Halliday GM, Middleton LT, Gentleman SM, Olson SH, Prusiner SB. 2018. MSA prions exhibit remarkable stability and resistance to inactivation. Acta Neuropathol 135:49–63. https://doi.org/10.1007/s00401-017-1762-2

50. Fritschi SK, Cintron A, Ye L, Mahler J, Bühler A, Baumann F, Neumann M, Nilsson KPR, Hammarström P, Walker LC, Jucker M. 2014. Aβ seeds resist inactivation by formaldehyde. Acta Neuropathol. 128:477–484. https://doi.org/10.1007/s00401-014-1339-2

51. Becker K, Wang X, Vander Stel K, Chu Y, Kordower J, Ma J. 2018. Detecting alpha synuclein seeding activity in formaldehyde-fixed MSA patient tissue by PMCA. Mol Neurobiol 55:8728–8737. https://doi.org/10.1007/s12035-018-1007-y

52. Han JY, Park KJ, Park HC, Lee YR, Moore RA, Sohn HJ, Choi YP. 2023. Autoclave treatment fails to completely inactivate DLB alpha-synuclein seeding activity. Biochem Biophys Rep 34:101446. https://doi.org/10.1016/j.bbrep.2023.101446

53. Ernst DR, Race RE. 1993. Comparative analysis of scrapie agent inactivation methods. J Virol Methods 41:193–201. https://doi.org/10.1016/0166-0934(93)90126-c

54. Taylor DM. 2000. Inactivation of transmissible degenerative encephalopathy agents: a review. Vet J 159:10–17. https://doi.org/10.1053/tvjl.1999.0406

55. Race RE, Raymond GJ. 2004. Inactivation of transmissible spongiform encephalopathy (prion) agents by environ LpH. J Virol 78:2164–2165. https://doi.org/10.1128/jvi.78.4.2164-2165.2004

56. Baune C, Groveman BR, Hughson AG, Thomas T, Twardoski B, Priola S, Chesebro B, Race B. 2023. Efficacy of Wex-cide 128 disinfectant against multiple prion strains. PLoS One 18:e0290325. https://doi.org/10.1371/journal.pone.0290325

57. Baune C, Wolfe LL, Schott KC, Griffin KA, Hughson AG, Miller MW, Race B. 2021. Reduction of chronic wasting disease prion seeding activity following digestion by mountain lions. mSphere 6:e0081221. https://doi.org/10.1128/msphere.00812-21

58. Hughson AG, Race B, Kraus A, Sangaré LR, Robins L, Groveman BR, Saijo E, Phillips K, Contreras L, Dhaliwal V, Manca M, Zanusso G, Terry D, Williams JF, Caughey B. 2016. Inactivation of prions and amyloid seeds with hypochlorous acid. PLoS Pathog 12:e1005914. https://doi.org/10.1371/journal.ppat.1005914

59. Peretz D, Supattapone S, Giles K, Vergara J, Freyman Y, Lessard P, Safar JG, Glidden DV, McCulloch C, Nguyen H-O, Scott M, Dearmond SJ, Prusiner SB. 2006. Inactivation of prions by acidic sodium dodecyl sulfate. J Virol 80:322–331. https://doi.org/10.1128/JVI.80.1.322-331.2006

60. Kimberlin RH, Walker CA, Millson GC, Taylor DM, Robertson PA, Tomlinson AH, Dickinson AG. 1983. Disinfection studies with two strains of mouse-passaged scrapie agent. J Neurol Sci 59:355–369. https://doi.org/10.1016/0022-510X(83)90021-7

61. Holec SAM, Block AJ, Bartz JC. 2020. The role of prion strain diversity in the development of successful therapeutic treatments. Prog Mol Biol Transl Sci 175:77–119. https://doi.org/10.1016/bs.pmbts.2020.07.001

62. Duffy P, Wolf J, Collins G, DeVoe AG, Streeten B, Cowen D. 1974. Possible person-to-person transmission of Creutzfeldt-Jakob disease. N Engl J Med 290:692–693. https://doi.org/10.1056/NEJM197403212901220

63. Brown P, Preece M, Brandel J-P, Sato T, McShane L, Zerr I, Fletcher A, Will RG, Pocchiari M, Cashman NR, d'Aignaux JH, Cervenáková L, Fradkin J, Schonberger LB, Collins SJ. 2000. Iatrogenic Creutzfeldt–Jakob disease at the millennium. Neurology 55:1075–1081. https://doi.org/10.1212/WNL.55.8.1075

64. d'Aignaux JH, Costagliola D, Maccario J, de Villemeur TB, Brandel JP, Deslys JP, Hauw JJ, Chaussain JL, Agid Y, Dormont D, Alpérovitch A. 1999. Incubation period of Creutzfeldt–Jakob disease in human growth hormone recipients in France. Neurology 53:1197–1197. https://doi.org/10.1212/WNL.53.6.1197

65. Masson C, Delalande I, Deslys JP, Hénin D, Fallet-Bianco C, Dormont D, Leys D. 1994. Creutzfeldt-Jakob disease after pituitary-derived human growth hormone therapy: two cases with valine 129 homozygous genotype. Neurology 44:179–180. https://doi.org/10.1212/wnl.44.1.179

66. Marzewski DJ, Towfighi J, Harrington MG, Merril CR, Brown P. 1988. Creutzfeldt-Jakob disease following pituitary-derived human growth hormone therapy: a new American case. Neurology 38:1131–1133. https://doi.org/10.1212/wnl.38.7.1131

67. Hannah EL, Belay ED, Gambetti P, Krause G, Parchi P, Capellari S, Hoffman RE, Schonberger LB. 2001. Creutzfeldt–Jakob disease after receipt of a previously unimplicated brand of dura mater graft. Neurology 56:1080–1083. https://doi.org/10.1212/WNL.56.8.1080

68. Shimizu S, Hoshi K, Muramoto T, Homma M, Ironside JW, Kuzuhara S, Sato T, Yamamoto T, Kitamoto T. 1999. Creutzfeldt-Jakob disease with florid-type plaques after cadaveric dura mater grafting. Arch Neurol 56:357. https://doi.org/10.1001/archneur.56.3.357

69. Antoine JC, Michel D, Bertholon P, Mosnier JF, Laplanche JL, Beaudry P, Hauw JJ, Veyret C. 1997. Creutzfeldt‐Jakob disease after extracranial dura mater embolization for a nasopharyngeal angiofibroma. Neurology 48:1451–1453. https://doi.org/10.1212/WNL.48.5.1451

70. Esmonde T, Lueck CJ, Symon L, Duchen LW, Will RG. 1993. Creutzfeldt-Jakob disease and lyophilised dura mater grafts: report of two cases. J Neurol Neurosurg Psychiatry 56:999–1000. https://doi.org/10.1136/jnnp.56.9.999

71. Willison HJ, Gale AN, McLaughlin JE. 1991. Creutzfeldt-Jacob disease following cadaveric dura mater graft. J Neurol Neurosurg Psychiatry 54:940. https://doi.org/10.1136/jnnp.54.10.940

72. Nisbet TJ, MacDonaldson I, Bishara SN. 1989. Creutzfeldt-Jakob disease in a second patient who received a cadaveric dura mater graft. JAMA 261:1118. https://doi.org/10.1001/jama.1989.03420080032008

73. Diringer H, Braig HR. 1989. Infectivity of unconventional viruses in dura mater. Lancet 1:439–440. https://doi.org/10.1016/s0140-6736(89)90035-4

74. Jaunmuktane Z, Mead S, Ellis M, Wadsworth JDF, Nicoll AJ, Kenny J, Launchbury F, Linehan J, Richard-Loendt A, Walker AS, Rudge P, Collinge J, Brandner S. 2015. Evidence for human transmission of amyloid-β pathology and cerebral amyloid angiopathy. Nature 525:247–250. https://doi.org/10.1038/nature15369

75. Purro SA, Farrow MA, Linehan J, Nazari T, Thomas DX, Chen Z, Mengel D, Saito T, Saido T, Rudge P, Brandner S, Walsh DM, Collinge J. 2018. Transmission of amyloid-β protein pathology from cadaveric pituitary growth hormone. Nature 564:415–419. https://doi.org/10.1038/s41586-018-0790-y

76. Belay ED, Blase J, Sehulster LM, Maddox RA, Schonberger LB. 2013. Management of neurosurgical instruments and patients exposed to Creutzfeldt-Jakob disease. Infect Control Hosp Epidemiol 34:1272–1280. https://doi.org/10.1086/673986

77. Will RG. 2003. Acquired prion disease: iatrogenic CJD, variant CJD, kuru. Br Med Bull 66:255–265. https://doi.org/10.1093/bmb/66.1.255

78. Laurenson IF, Whyte AS, Fox C, Babb JR. 1999. Contaminated surgical instruments and variant Creutzfeldt-Jakob disease. Lancet 354:1823. https://doi.org/10.1016/s0140-6736(05)70594-8

79. Collins S, Law MG, Fletcher A, Boyd A, Kaldor J, Masters CL. 1999. Surgical treatment and risk of sporadic Creutzfeldt-Jakob disease: a case-control study. Lancet 353:693–697. https://doi.org/10.1016/s0140-6736(98)08138-0

80. de Pedro-Cuesta J, Mahillo-Fernández I, Rábano A, Calero M, Cruz M, Siden A, Laursen H, Falkenhorst G, Mølbak K, Group ER. 2011. Nosocomial transmission of sporadic Creutzfeldt-Jakob disease: results from a risk-based assessment of surgical interventions. J Neurol Neurosurg Psychiatry 82:204–212. https://doi.org/10.1136/jnnp.2009.188425

81. Brandel J-P, Vlaicu MB, Culeux A, Belondrade M, Bougard D, Grznarova K, Denouel A, Plu I, Bouaziz-Amar E, Seilhean D, Levasseur M, Haïk S. 2020. Variant Creutzfeldt–Jakob disease diagnosed 7.5 years after occupational exposure. N Engl J Med 383:83–85. https://doi.org/10.1056/NEJMc2000687

82. Casassus B. 2021. France halts prion research amid safety concerns. Science 373:475–476. https://doi.org/10.1126/science.373.6554.475

83. Baron H, Safar J, Groth D, DeArmond SJ, Prusiner SB. 1999. Biosafety issues in prion diseases, p 743–777. In Prusiner SB (ed), Prion biology and diseases. Cold Spring Harbor Laboratory Press, Cold Spring Harbor.

84. Flechsig E, Hegyi I, Enari M, Schwarz P, Collinge J, Weissmann C. 2001. Transmission of scrapie by steel-surface-bound prions. Mol Med 7:679–684. https://doi.org/10.1007/BF03401958

85. Zobeley E, Flechsig E, Cozzio A, Enari M, Weissmann C. 1999. Infectivity of scrapie prions bound to a stainless steel surface. Mol Med 5:240–243. https://doi.org/10.1007/BF03402121

86. Williams K, Hughson AG, Chesebro B, Race B. 2019. Inactivation of chronic wasting disease prions using sodium hypochlorite. PLoS One 14:e0223659. https://doi.org/10.1371/journal.pone.0223659

87. Dickinson AG, Fraser H, Outram GW. 1975. Scrapie incubation time can exceed natural lifespan. Nature 256:732–733. https://doi.org/10.1038/256732a0

88. Klöhn P-C, Stoltze L, Flechsig E, Enari M, Weissmann C. 2003. A quantitative, highly sensitive cell-based infectivity assay for mouse scrapie prions. Proc Natl Acad Sci U S A 100:11666–11671. https://doi.org/10.1073/pnas.1834432100

89. Edgeworth JA, Jackson GS, Clarke AR, Weissmann C, Collinge J. 2009. Highly sensitive, quantitative cell-based assay for prions adsorbed to solid surfaces. Proc Natl Acad Sci U S A 106:3479–3483. https://doi.org/10.1073/pnas.0813342106

90. Atarashi R, Satoh K, Sano K, Fuse T, Yamaguchi N, Ishibashi D, Matsubara T, Nakagaki T, Yamanaka H, Shirabe S, Yamada M, Mizusawa H, Kitamoto T, Klug G, McGlade A, Collins SJ, Nishida N. 2011. Ultrasensitive human prion detection in cerebrospinal fluid by real-time quaking-induced conversion. Nat Med 17:175–178. https://doi.org/10.1038/nm.2294

91. Wilham JM, Orrú CD, Bessen RA, Atarashi R, Sano K, Race B, Meade-White KD, Taubner LM, Timmes A, Caughey B. 2010. Rapid end-point quantitation of prion seeding activity with sensitivity comparable to bioassays. PLoS Pathog 6:e1001217. https://doi.org/10.1371/journal.ppat.1001217

92. Rossi M, Candelise N, Baiardi S, Capellari S, Giannini G, Orrù CD, Antelmi E, Mammana A, Hughson AG, Calandra-Buonaura G, Ladogana A, Plazzi G, Cortelli P, Caughey B, Parchi P. 2020. Ultrasensitive RT-QuIC assay with high sensitivity and specificity for Lewy body-associated synucleinopathies. Acta Neuropathol 140:49–62. https://doi.org/10.1007/s00401-020-02160-8

93. Metrick MA, do Carmo Ferreira N, Saijo E, Hughson AG, Kraus A, Orrú C, Miller MW, Zanusso G, Ghetti B, Vendruscolo M, Caughey B. 2019. Million-fold sensitivity enhancement in proteopathic seed amplification assays for biospecimens by Hofmeister ion comparisons. Proc Natl Acad Sci U S A 116:23029–23039. https://doi.org/10.1073/pnas.1909322116

94. Saijo E, Ghetti B, Zanusso G, Oblak A, Furman JL, Diamond MI, Kraus A, Caughey B. 2017. Ultrasensitive and selective detection of 3-repeat tau seeding activity in Pick disease brain and cerebrospinal fluid. Acta Neuropathol 133:751–765. https://doi.org/10.1007/s00401-017-1692-z

95. Atarashi R, Moore RA, Sim VL, Hughson AG, Dorward DW, Onwubiko HA, Priola SA, Caughey B. 2007. Ultrasensitive detection of scrapie prion protein using seeded conversion of recombinant prion protein. Nat Methods 4:645–650. https://doi.org/10.1038/nmeth1066

96. Orrú CD, Groveman BR, Hughson AG, Barrio T, Isiofia K, Race B, Ferreira NC, Gambetti P, Schneider DA, Masujin K, Miyazawa K, Ghetti B, Zanusso G, Caughey B. 2024. Sensitive detection of pathological seeds of α-synuclein, tau and prion protein on solid surfaces. PLoS Pathog 20:e1012175. https://doi.org/10.1371/journal.ppat.1012175

97. Yuan Q, Rowden G, Wolf TM, Schwabenlander MD, Larsen PA, Bartelt-Hunt SL, Bartz JC. 2022. Sensitive detection of chronic wasting disease prions recovered from environmentally relevant surfaces. Environ Int 166:107347. https://doi.org/10.1016/j.envint.2022.107347

98. Christenson PR, Li M, Rowden G, Larsen PA, Oh SH. 2023. Nanoparticle-enhanced RT-QuIC (Nano-QuIC) diagnostic assay for misfolded proteins. Nano Lett 23:4074–4081. https://doi.org/10.1021/acs.nanolett.3c01001

99. Hartley EG. 1967. Action of disinfectants on experimental mouse scrapie. Nature 213:1135. https://doi.org/10.1038/2131135a0

100. Chatigny MA, Prusiner SB. 1979. Biohazards and risk assessment of laboratory studies on the agents causing the spongiform encephalopathies, p 491–514. In Prusiner SB, Hadlow WJ (ed), Slow transmissible diseases of the nervous system. Vol. 2. Academic Press, New York.

101. McDonnell G, Dehen C, Perrin A, Thomas V, Igel-Egalon A, Burke PA, Deslys JP, Comoy E. 2013. Cleaning, disinfection and sterilization of surface prion contamination. J Hosp Infect 85:268–273. https://doi.org/10.1016/j.jhin.2013.08.003

102. McNulty E, Nalls AV, Mellentine S, Hughes E, Pulscher L, Hoover EA, Mathiason CK. 2019. Comparison of conventional, amplification and bio-assay detection methods for a chronic wasting disease inoculum pool. PLoS One 14:e0216621. https://doi.org/10.1371/journal.pone.0216621

103. Shikiya RA, Bartz JC. 2011. In vitro generation of high-titer prions. J Virol 85:13439–13442. https://doi.org/10.1128/JVI.06134-11

104. Kincaid AE, Bartz JC. 2007. The nasal cavity is a route for prion infection in hamsters. J Virol 81:4482–4491. https://doi.org/10.1128/JVI.02649-06

105. Hoover CE, Davenport KA, Henderson DM, Pulscher LA, Mathiason CK, Zabel MD, Hoover EA. 2016. Detection and quantification of CWD prions in fixed paraffin embedded tissues by real-time quaking-induced conversion. Sci Rep 6:25098. https://doi.org/10.1038/srep25098

106. Orrù CD, Wilham JM, Vascellari S, Hughson AG, Caughey B. 2012. New generation QuIC assays for prion seeding activity. Prion 6:147–152. https://doi.org/10.4161/pri.19430

107. Haley NJ, Van de Motter A, Carver S, Henderson D, Davenport K, Seelig DM, Mathiason C, Hoover E. 2013. Prion-seeding activity in cerebrospinal fluid of deer with chronic wasting disease. PLoS One 8:e81488. https://doi.org/10.1371/journal.pone.0081488

108. Vascellari S, Orrù CD, Caughey B. 2022. Real-time quaking-induced conversion assays for prion diseases, synucleinopathies, and tauopathies. Front Aging Neurosci 14:853050. https://doi.org/10.3389/fnagi.2022.853050

109. Schmitz M, Cramm M, Llorens F, Müller-Cramm D, Collins S, Atarashi R, Satoh K, Orrù CD, Groveman BR, Zafar S, Schulz-Schaeffer WJ, Caughey B, Zerr I. 2016. The real-time quaking-induced conversion assay for detection of human prion disease and study of other protein misfolding diseases. Nat Protoc 11:2233–2242. https://doi.org/10.1038/nprot.2016.120

110. Reed LJ, Muench H. 1938. A simple method of estimating fifty per cent endpoints. Am J Epidemiol 27:493–497. https://doi.org/10.1093/oxfordjournals.aje.a118408